

Manipulating modern diesel engine particulate emission characteristics through butanol fuel blending and fuel injection strategies for efficient diesel oxidation catalysts

Fayad, Mohammed; Tsolakis, Athanasios; Fernandez-Rodriguez, David; Herreros, Jose; Francisco, Martos; Lapuerta, M

DOI:

[10.1016/j.apenergy.2016.12.102](https://doi.org/10.1016/j.apenergy.2016.12.102)

License:

Creative Commons: Attribution-NonCommercial-NoDerivs (CC BY-NC-ND)

Document Version

Peer reviewed version

Citation for published version (Harvard):

Fayad, M, Tsolakis, A, Fernandez-Rodriguez, D, Herreros, J, Francisco, M & Lapuerta, M 2017, 'Manipulating modern diesel engine particulate emission characteristics through butanol fuel blending and fuel injection strategies for efficient diesel oxidation catalysts', *Applied Energy*, vol. 190, pp. 490-500.

<https://doi.org/10.1016/j.apenergy.2016.12.102>

[Link to publication on Research at Birmingham portal](#)

Publisher Rights Statement:

Checked 17/02/2017

General rights

Unless a licence is specified above, all rights (including copyright and moral rights) in this document are retained by the authors and/or the copyright holders. The express permission of the copyright holder must be obtained for any use of this material other than for purposes permitted by law.

- Users may freely distribute the URL that is used to identify this publication.
- Users may download and/or print one copy of the publication from the University of Birmingham research portal for the purpose of private study or non-commercial research.
- User may use extracts from the document in line with the concept of 'fair dealing' under the Copyright, Designs and Patents Act 1988 (?)
- Users may not further distribute the material nor use it for the purposes of commercial gain.

Where a licence is displayed above, please note the terms and conditions of the licence govern your use of this document.

When citing, please reference the published version.

Take down policy

While the University of Birmingham exercises care and attention in making items available there are rare occasions when an item has been uploaded in error or has been deemed to be commercially or otherwise sensitive.

If you believe that this is the case for this document, please contact UBIRA@lists.bham.ac.uk providing details and we will remove access to the work immediately and investigate.

Download date: 24. Apr. 2024

1 **Manipulating modern diesel engine particulate emission characteristics through butanol fuel** 2 **blending and fuel injection strategies for efficient diesel oxidation catalysts**

3 **M.A. Fayad^{a,b}, A. Tsolakis^{a*}, D. Fernández-Rodríguez^c, J.M. Herreros^{a,d}, F.J. Martos^e, and M. Lapuerta^c**

4 ^a School of Mechanical Engineering, University of Birmingham, Birmingham B15 2TT, UK

5 ^b Energy and Renewable Energies Technology Center, University of Technology, Baghdad, Iraq

6 ^c University of Castilla-La Mancha, Escuela Técnica Superior de Ingenieros Industriales, Edificio Politécnico. Avda.
7 Camilo José Cela s/n, 13071 Ciudad Real, Spain

8 ^d Faculty of Engineering, Environment & Computing, Coventry University, Coventry. CV1 5FB, UK

9 ^e Escuela Técnica Superior de Ingeniería Industrial, University of Málaga, 29071, Málaga, Spain

10 * Corresponding author. Email: a.tsolakis@bham.ac.uk, tel.: +44 (0) 121 414 4170;

11 **Abstract**

12 Decoupling the dependences between emission reduction technologies and engine fuel economy in
13 order to improve them both simultaneously has been proven a major challenge for the vehicle
14 research communities. Additionally, the lower exhaust gas temperatures associated with the modern
15 and future generation internal combustion engines are challenging the performance of road transport
16 environmental catalysts. Studying how fuel properties and fuel injection strategies affect the
17 combustion characteristics, emissions formation and hence catalysts performance can unveil
18 synergies that can benefit vehicle emissions and fuel economy and as well as guide the design of
19 next generation sustainable fuels. The experimental work presented here was conducted using a
20 modern single-cylinder, common rail fuel injection system diesel engine equipped with a diesel
21 oxidation catalyst (DOC). The impact of the fuel post-injection strategy that is commonly used as
22 part of the aftertreatment system function (i.e. regeneration of diesel particulate filters or activity in
23 hydrocarbon selective reduction of NO_x), combined with butanol-diesel fuel blend (B20)
24 combustion on engine emissions formation, particulate matter characteristics (size distribution,
25 morphology and structure) and oxidation catalyst activity were studied. It was found that post-
26 injection produced lower PM concentration and modified the soot morphological parameters by
27 reducing the number of primary particles (n_{po}), the radius of gyration (R_g), and the fractal dimension
28 (D_f). The results were compared with the engine operation on diesel fuel. The increased
29 concentration of HC and CO in the exhaust as a result of the diesel fuel post-injection at the studied
30 exhaust conditions (i.e. T= 300 °C) led in the reduction of the DOC activity due to the increased
31 competition of species for active sites. This effect was improved the combustion of B20 when
32 compared to diesel.

33 **Keywords:** alternative fuels, diesel oxidation catalyst, gaseous emissions, particulate matter, post-
34 injection, butanol

35 1. Introduction

36 With the view to improve the air quality, new engine and vehicle systems and technologies
37 are under development in order to reduce pollutants emitted to the atmosphere especially in the very
38 challenging transportation sector [1, 2]. In road transport, replacing fossil fuels with biofuels also
39 provide cleaner combustion and consequently improve the efficiency of the catalytic aftertreatment
40 systems and can be considered as a way to help vehicle manufacturers to achieve the emissions
41 legislative limits such as the EURO 6 and CARB (LEV III) [3].

42 Bioalcohols and other oxygenated fuels have been reported to reduce emissions, when
43 replacing gasoline fuels in spark-ignition (SI) engines. More recently these fuels have been studied
44 as substitute to diesel fuel [4-8] because of their oxygen content that contributes in the reduction of
45 the engine out CO, UHC (unburned hydrocarbons), NO_x (nitrogen oxides) and total PM emissions.
46 It is reported that the hydroxyl group present in alcohols is more efficient in reducing diesel engine
47 PM than other functional groups with the same oxygen content, especially at high engine loads [9-
48 11]. The combustion of diesel-ethanol blends for example has been widely reported to reduce PM
49 emissions [4, 12]. However, there are also drawbacks [13, 14] such as the ethanol's limited solubility
50 in diesel fuel [15], the very low cetane number and the lower dynamic viscosity, parameters that can
51 impact on the engine's operation and combustion characteristics [4, 16, 17]. Butanol in diesel has
52 shown more promising characteristics as an alternative fuel to ethanol [4] due to higher cetane
53 number and better solubility in diesel fuel as a consequence of being less polar than other alcohols
54 with shorter chain. Furthermore, it has higher heating value, lower volatility, and less hydrophilic
55 character [18, 19].

56 Modern engine after-treatment systems consist of different components such as the diesel
57 oxidation catalysts (DOC) and diesel particulate filters (DPF) [20]. DOCs have a honeycomb
58 monolith shape with high cell density (large surface area) and suitable loadings of a catalytic
59 material such as platinum and/or palladium that is able to almost eliminate CO, HC and much of the
60 particulate organic fraction [16, 20, 21]. DOC also oxidise NO to produce NO₂ that can then be
61 utilised in the DPF to passively oxidise soot at low temperatures [16, 22, 23]. The DOC's activity
62 depends on exhaust gas temperature, residence time of the exhaust gas in the catalyst, level and
63 nature of gaseous and particulate matter exhaust species and inhibitions/synergies between the
64 different species contained in the exhaust gas [23, 24]. In the same way, DPF performance is also
65 influenced by size and morphology [fractal dimension (D_f), radius of gyration (R_g) and number of
66 primary particles (n_{po})] of soot particles making understand their control challenging [16, 25].
67 Therefore, the effect of fuel and engine operating parameters such as injection settings (e.g. number
68 of injections, injection timing, injection pressure, injection quantity) needs to be understood in order
69 to improve not only the engine performance (power/torque) characteristics but also the function of

70 the aftertreatment system [26]. Several studies have shown that the post-injection in combination
71 with the DOC is commonly used to increase the exhaust gas temperature in order to aid the DPF
72 regeneration (i.e. active regeneration) [27].

73 The impact of fuel post-injection on engine out gaseous emissions and PM has also been
74 investigated [28-30]. The temperature increase late in the combustion cycle due to the post-fuel
75 injection, which can enhance soot oxidation, produced during the main combustion event [30-34],
76 but this is reported to be dependent on the engine calibration and operation conditions. Some studies
77 have reported PM increase with post-injection at high engine loads and speeds [28]. In some cases
78 post-injection also contributes in the reduction of engine out NO_x due to the formation of nitrated-
79 hydrocarbons through the reactions of NO_x with HC radicals [35, 36]. It is reported that CO and
80 THC are reduced with post-injection and sharply increased with later post-injection timing (after 70
81 CAD ATDC) [27]. Late combustion caused by post-injection increases the level of THC emissions
82 as the late injected fuel is not burnt in the combustion chamber [26, 29, 37]. In this way, HCs are
83 oxidized in the DOC, increasing considerably the temperature of the exhaust upstream of the DPF
84 and trapping a high proportion of the soot flowing in the exhaust stream [27, 38, 39]. It is
85 documented that the main-post-injection increases the rate of soot oxidation in the combustion cycle
86 due to the enhancement of the gas mean temperature and air/fuel mixing, which leads to the
87 reduction in number and diameter of primary particles [40, 41].

88 Combined advances in alternative fuels and aftertreatment systems are required in order to
89 fulfil the stringent emission regulations and also help in decoupling mutual dependences between
90 pollutants control and engine fuel economy. Most of the studies on alternative fuels combustion
91 published in the literature are focused on the effect of the fuel on the engine performance and on the
92 engine emissions, including PM characteristics [17] which influences passive and active DPF
93 regeneration [20] as well as DPF trapping efficiency [42, 43]. Recent studies have reported work on
94 gaseous emissions interactions [22] and the influence of PM characteristics [16] (size and shape)
95 emitted from the combustion of different fuels on the DOC performance. However, there is still
96 scarce information regarding the effect of alternative fuels (e.g. alcohol blends) on both, PM
97 characteristics and DOC activity with simultaneous use of fuel post-injection, strategy that is
98 required in diesel vehicles for catalyst heat-up in active and DPF regeneration. Therefore, the aim of
99 this research work focuses on the role of the fuel post-injection and diesel-butanol fuel blends
100 combustion on PM characteristics (number, size, morphology) and the impact on the DOC activity.
101 The DOC catalyst activity was assessed under the same temperature, space velocity and pressure
102 conditions with the only comparative parameter being the exhaust gas composition.

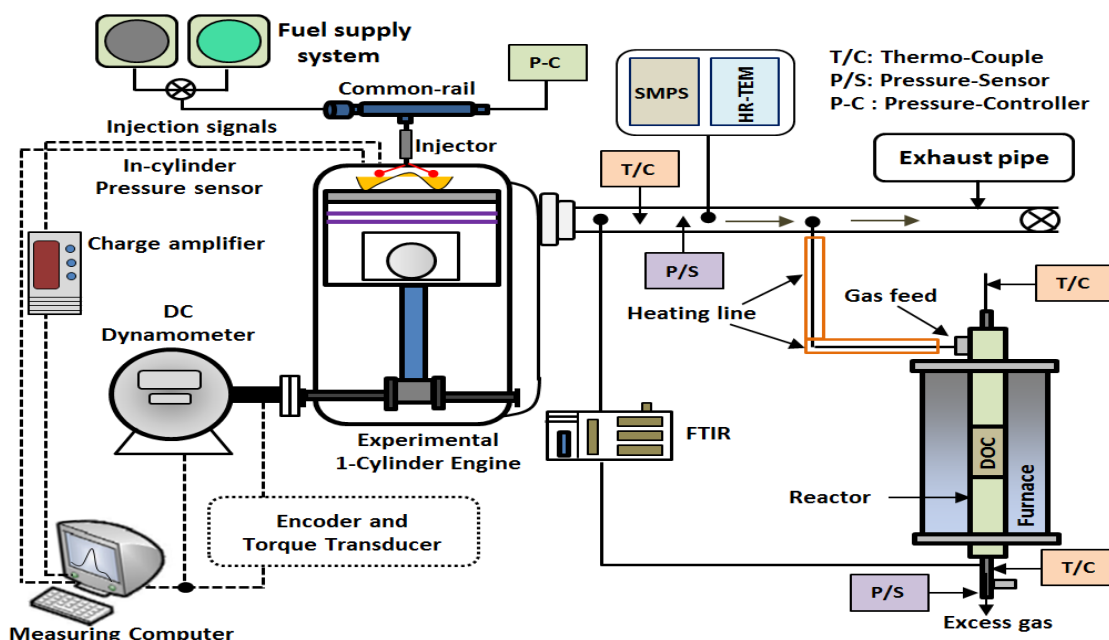
103 **2. Experimental setup and materials**

104 A modern single-cylinder, water-cooled, common rail fuel injection system, four-stroke
 105 experimental diesel engine was employed in this investigation. The engine used in this study is
 106 a single cylinder research engine that was designed by the investigators and incorporates one of the
 107 cylinder heads of a V6 production engine. The main specifications of the test engine can be found in
 108 Table 1. A schematic diagram of the experimental set up is shown in Figure 1. The diesel oxidation
 109 catalyst studies were carried out using one inch in diameter monolith catalyst that was placed in a
 110 reactor inside a furnace where the temperature and the engine exhaust gas flow can be controlled by
 111 a thermocouple (located upstream the catalyst) and a flow meter respectively.

112 **Table 1.** Research engine specifications.

Engine parameters	Specifications
Engine type	Diesel 1- Cylinder
Stroke Type	Four-Stroke
Cylinder Bore x Stroke (mm)	84 x 90
Connecting Rod Length (mm)	160
Compression Ratio	16.1
Displacement (cc)	499
Engine Speed Range (rpm)	900 – 2000
IMEP Range (bar)	< 7
Fuel Pressure Range (bar)	500 – 1500
Number of Injections	3 injection events

113



114

115 **Figure 1.** Schematic diagram of test platform and sampling system.

116 The Ultra Low Sulphur Diesel (ULSD) fuel used for the study was supplied by Shell Global
 117 Solutions UK. Butanol was purchased from Fisher Scientific Company and used in this study for the

118 diesel-butanol blends. The ULSD, butanol and fuel blend properties are presented in Table 2. The
 119 particular diesel fuel used in this research as reference fuel was selected without any biodiesel
 120 (thereby with zero oxygen content) in its composition, in order to study the effect of the oxygen in
 121 the combustion process when diesel fuel is blended with butanol. The diesel-butanol blend (B20) is a
 122 mix of 80% diesel and 20% butanol (%Vol.).

123 **Table 2.** Fuels specification [4, 16].

Properties	Method	ULSD	Butanol	B20D80
Cetane number	ASTM D7668-14	50.2	17	41.98
Latent heat of vaporization (kJ/kg)		243	585	-
Bulk modulus (MPa)		1410	1500	-
Density at 15 °C (kg/m ³)	EN 12185	840.4	809.5	833.2
Upper heating value (MJ/kg)		45.76	36.11	43.5
Lower heating value (MJ/kg)		43.11	33.12	40.91
Water content by coulometric KF (mg/kg)	EN 12937	40	170	389.4
Kinematic viscosity at 40 °C (cSt)	EN ISO 3104	2.564	2.23	2.27
Lower Calorific Value (MJ/kg)		43.11	33.12	39.95
Lubricity at 60 °C(μm)	EN ISO 12156	424	571.15	444.5
Fatty acid methyl ester % (v/v)	NF EN 14078-A	<0.05		
Cold filter plugging point (CFPP)	ASTM D-6371	-18	<-51	-18
C (wt %)		86.44	64.78	81.56
H (wt %)		13.56	13.63	13.35
O (wt %)		0	21.59	4.318

124 At significantly lower or higher than 300 °C exhaust gas temperatures; the impact of fuels and
 125 post injection strategy on the DOC may not be as robust and conclusive as the catalyst may not light-
 126 off (low load) or the activity may not be affected (high loads). All tests were performed under a
 127 constant engine speed of 1800 rpm with an engine load of 3 bar IMEP (Indicated Mean Effective
 128 Pressure). An AVL GH13P was used to record the in-cylinder pressure [44]. The charge from the
 129 pressure transducer (mounted in the cylinder head) was amplified by an AVL FlexiFEM 2P2
 130 Amplifier [45]. A digital shaft encoder producing 360 pulses per revolution was used to measure the
 131 crank shaft position. The data from the crank shaft position and pressure was combined to create an
 132 in-cylinder pressure trace. The engine is equipped with common-rail fuel injection system which
 133 allows the control of multiple injection events. The injection was split in pre, main, and post fuel
 134 injection with injection timing of 15 and 3 deg bTDC and 60 deg aTDC, injection pressure of 650
 135 bar, and post-injection duration of 0.1 ms. A bespoke experimental facility was used in this study
 136 that was designed to assess the performance of catalysts and combination of aftertreatment systems
 137 under real engine exhaust gas while providing flexibility with temperatures and reductants (i.e.
 138 hydrocarbons, ammonia, hydrogen) selection. The DOC used in this study was supplied by Johnson
 139 Matthey Plc and was positioned inside a mini reactor that was located inside a furnace and was fed

140 with real engine exhaust gas. The temperature upstream the DOC was monitored using K-type
141 thermocouples. The temperature of the reactor inside a tubular furnace was set at 300 °C while
142 maintaining constant gas hourly space velocity (GHSV) of 35000 h⁻¹. The details of the catalyst
143 (DOC) used in this study was a 4.237 kg/m³ with optimal platinum:palladium proportion (weight
144 ratio 1:1) with alumina and zeolite washcoat (158.66 kg/m³ loading). The total dimensions of the
145 DOC were 25.4 mm diameter, 91.4 mm length, and 4.3 mil wall thickness of the DOC [16, 22, 23].

146 A MultiGas 2030 FTIR spectrometry based analyzer was employed for exhaust gaseous
147 emissions measurement such as: carbon monoxide (CO), carbon dioxide (CO₂), nitrogen oxide (NO
148 and NO₂), nitrous oxide (N₂O), and individual hydrocarbons species such as methane (CH₄), ethane
149 (C₂H₆), ethylene (C₂H₄). Particulate Size Distributions (PSD) were analysed using a TSI 3080
150 scanning mobility particle sizer (SMPS). Exhaust gas part was sampled and diluted with air when
151 using the rotating disk thermodiluter (TSI 379020A) to control the dilution ratio. The dilution ratio
152 was set at 1:100 for all the tests and the thermodiluter temperature was 150 °C. The SMPS was
153 connected downstream of the dilution system in order to extract a diluted sample for the particle size
154 measurement.

155 Soot particles were collected from the exhaust pipe on a 3.05 mm diameter copper grids
156 attached to a sampling probe. The sampling tool and lines were cleaned with nitrogen before each
157 test to remove deposited soot particles. A Philips CM-200 high resolution transmission electron
158 microscopy (HR-TEM) with a resolution about 2 Å at an accelerating voltage of 200 kV was used to
159 analyse the particles. A digital image analysis software in Matlab was designed to calculate the
160 morphological parameters of the agglomerates (radius of gyration, R_g, number of primary particles,
161 n_{po}, and fractal dimension, D_f) [46, 47]. The conversion from pixels to nanometres was calibrated by
162 comparison with standard latex spheres shadowed with gold. For each condition, two grids and
163 minimum 33 photographs were taken per fuel to calculate the morphology parameters as well as
164 least 26 agglomerates were chosen for each condition and fuel to obtain the results. Furthermore,
165 more than 200 primary particles were manually and randomly selected from different aggregates to
166 determine an average diameter of primary particles and to produce the fitted normal distribution of
167 primary particles at each fuel and condition.

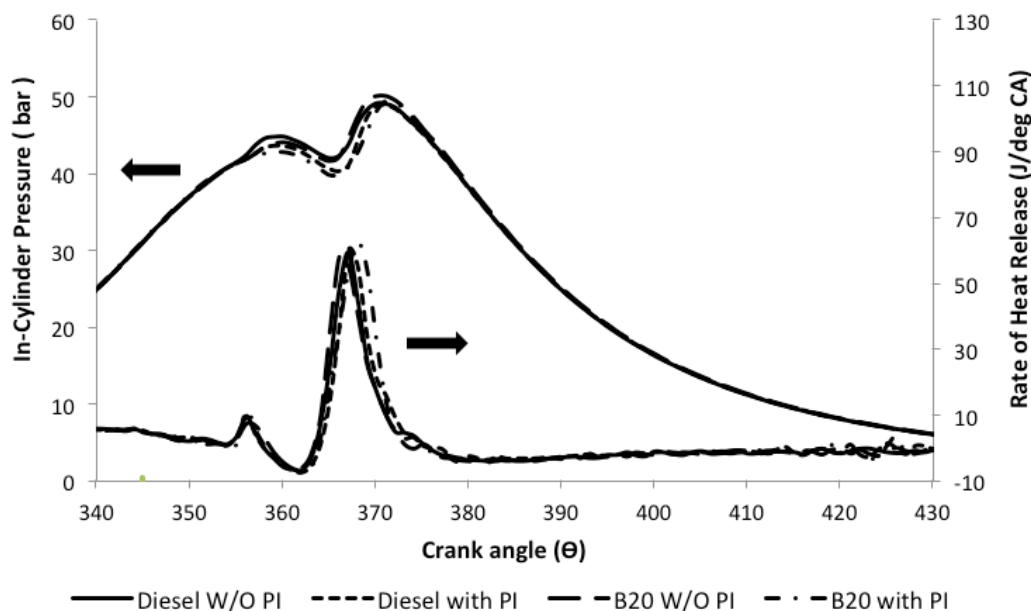
168 **3. Results and discussions**

169 **3.1 Combustion characteristics**

170 Figure 2 shows the effects of the injection strategy on the in-cylinder pressure and the rate of
171 heat release (ROHR) versus crank angle degree (CAD) for the combustion of diesel and B20. It has
172 to be noted that neither the post-injection nor the fuel properties notably affected the combustion
173 events. It is though that this is due to the effect of the pre-injection which thermally conditioned the

174 in-cylinder, thus minimizing the effect of the worse autoignition properties (Table 2) of the B20
 175 blend with respect to diesel fuel. Small increase of the in-cylinder pressure and heat release was
 176 obtained from the combustion of B20 that may also explain the changes in emissions later on.

177



178

179 **Figure 2.** Effect of fuel post-injection strategy and fuels structure on combustion characteristics.

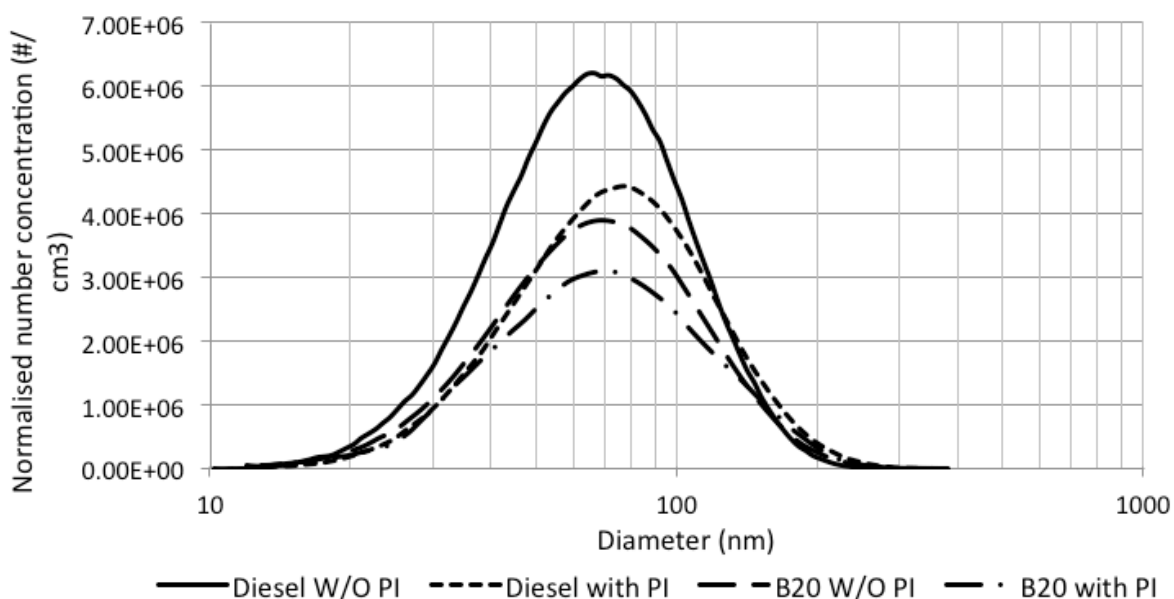
180 **3.2 Influence of fuel post-injection and fuel structure on engine out PM and gaseous emissions**

181 The PSDs were obtained upstream the DOC in order to understand the influence of B20 and
 182 post-injection on the particle formation and oxidation processes. The combustion of the alcohol
 183 blend (B20) reduced the number of particles along the whole distribution with respect to combustion
 184 of the diesel fuel with and without post-injection (Figure 3). A slight reduction is observed in the
 185 average particle diameter, from 94 nm for diesel down to 64 nm for B20 in the absence of post-
 186 injection. These results are in agreement with previous studies of butanol-diesel blends combustion
 187 [16, 48] justified by the presence of the hydroxyl group in the butanol molecule [16] leading to lower
 188 rates of PM formation [4, 16] and to enhanced PM oxidation rates [16, 49]. Reductions of the soot in
 189 the exhaust are often reported when post-injection is introduced due to increased expansion
 190 temperature and enhanced mixing within the cylinder that increases oxidation of soot produced from
 191 the main injection [30, 32-34]. The maximum number concentration, MMD, and sigma g in Figure 3
 192 are presented in Table 3 for diesel fuel and B20.

193 **Table 3.** Maximum number concentration, MMD and sigma g for diesel and B20.

194

	Diesel W/O PI	Diesel with PI	B20 W/O PI	B20 with PI
Max. number concentration (#/cm ³)	6.23E6	4.45E6	3.90E6	3.10E6
MMD (nm)	74.81	79.71	73.96	76.53
Sigma g	6.41	5.82	4.76	4.13



195

196

Figure 3. Effect of post-injection on particle size distribution for diesel and B20 fuels.

197

198

199

200

201

202

203

204

205

206

207

208

209

210

211

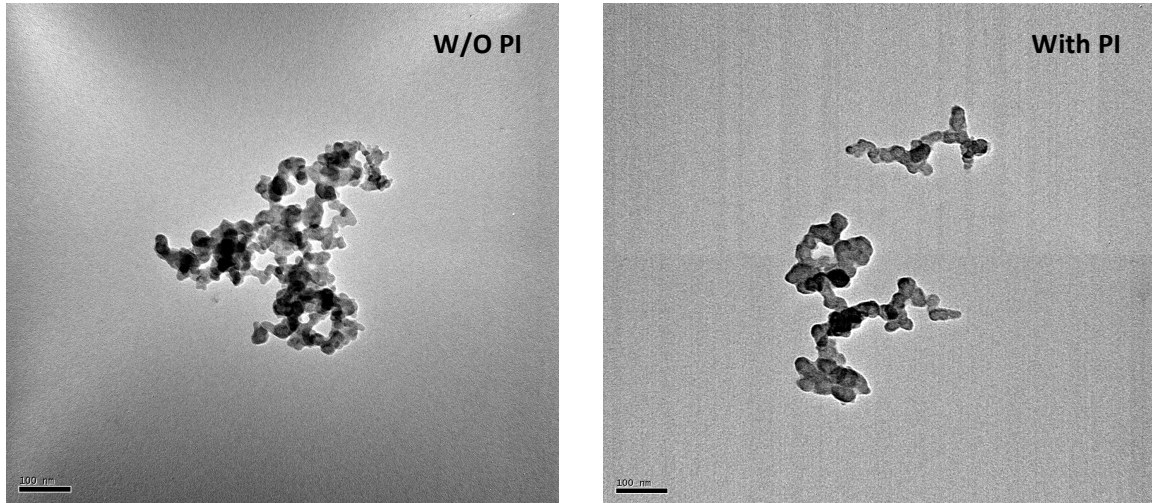
212

213

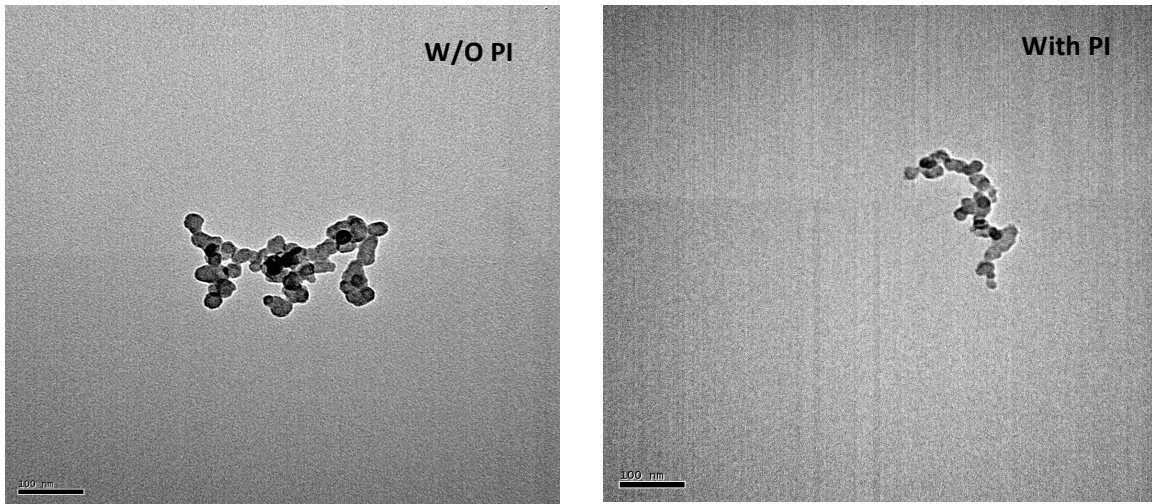
214

215

The particles emitted from diesel engine have a variety of shapes and sizes and consist of tens to hundreds of primary particles agglomerated together, forming irregular clusters [50, 51]. Figure 4 depicts representative examples of HR-TEM micrographs from particles sampled from the exhaust gas at the different conditions studied in this research. PM morphological parameters (radius of gyration (R_g), number of primary particles (n_{po}) and fractal dimension (D_f)) for Diesel and B20 are calculated from the obtained HR-TEM images (Figure 4). Trends observed in these representative examples are in agreement with the statistical trends discussed below. Figure 5 shows the results of the average particles electrical mobility diameter obtained with SMPS jointly with soot's average radius of gyration and number of primary particles. According to these results the average agglomerate size (quantified by radius of gyration and mobility diameter) and the number of primary particles are lower for B20 than for diesel fuel independently of the injection strategy. It is believed that for diesel combustion the enhanced net formation rate of particles increases the likelihood of collisions and further aggregation leading to higher number of primary particles. It is thought that oxygen content in butanol blend (B20) improves the soot oxidation [52] while the incorporation of the post-injection leads to enhanced oxidation resulting in the disappearance of a fraction of the primary particles already formed (Figure 5). The reduction in number of particles as measured by the SMPS and the reduction in number of primary particles in the particle aggregate for B20 are also associated with the reduction in the formation of soot precursors due to the chemical structure of butanol and the lack of PAH in butanol, besides the effect of the oxygen content of butanol.

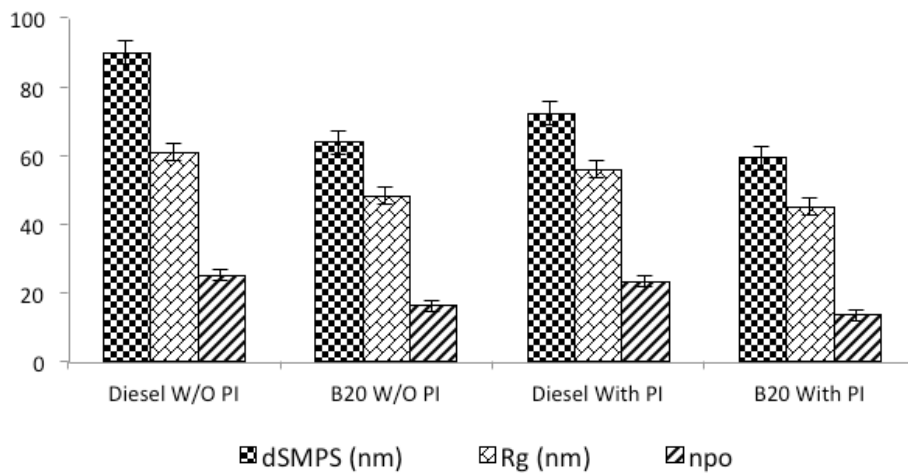


(a)



(b)

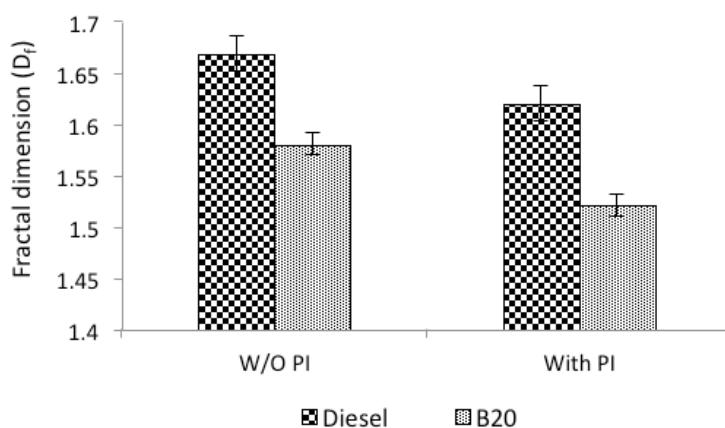
216 **Figure 4.** Typical examples of HR-TEM micrograph of particles matter collected at the exhaust gas
 217 for (a) diesel fuel, and (b) B20.



218

219 **Figure 5.** Effect of fuel injection strategy and fuel characteristics on particle size from SMPS, radius
 220 of gyration (R_g) and number of primary particles (n_{po}).

221 The influence of the fuel and injection strategy (with and without post-injection) on the
 222 fractal dimension (D_f) is shown in Figure 6. The fractal dimension of the agglomerates produced
 223 from the diesel fuel is higher (by 0.09) than that from B20 for both injection strategies (Figure 6) and
 224 this is in agreement with the work described by both Fayad et al. [16] and Choi et al. [53]. As a
 225 general rule [54] a reduction of the fractal dimension should be expected when there is a high
 226 concentration of particles as a result of the increased likelihood of collisions between agglomerates.
 227 However, in the case of agglomerates from oxygenated fuels, despite the lower particle
 228 concentration (and the consequent reduced likelihood of collisions) fractal dimensions were not
 229 found to be higher, but were systematically lower instead, probably due to some internal oxidation of
 230 agglomerates occurring after being formed. Similarly, the fractal dimension is also lower when post-
 231 injection was introduced for both fuels, despite the higher particle concentration also in this case
 232 (Figure 6). A conceptual model is suggested here to justify these trends. In the early stage of nuclei
 233 and primary particle formation fractal dimension is close to 3 and the primary particle size
 234 continuously increases (spherical nuclei and spherical primary particles). Collisions between
 235 particles and agglomerates and between agglomerates and agglomerates will increase the size of the
 236 agglomerate and reduce their fractal dimension (particle growth dominant over particle oxidation).
 237 This phenomenon will be more intense in the case of diesel without post injection conditions due to
 238 the higher rate of particle formation. Afterwards, the oxidation of particles will become dominant
 239 over the particle formation and the size of both primary particles and agglomerates could decrease,
 240 while the fractal dimension will deeply decrease, for the reason pointed out above. In this case, the
 241 decrease in fractal dimension will be more intense for the case of oxygenated fuels and post-
 242 injection conditions. Therefore, it is speculated that the resultant agglomerates from oxygenate fuels
 243 and post-injection conditions will have lower fractal dimension as the oxidation will remain being
 244 the dominant mechanism in front of particle formation and growth for longer time, as a consequence
 245 of the enhanced reactivity of soot particles (in the case of oxygenated fuels/) or of the enhanced
 246 temperature conditions in the exhaust flow (in the case of post-injection). More research and some
 247 in-cylinder sampling techniques should be used for a more comprehensive justification.



248

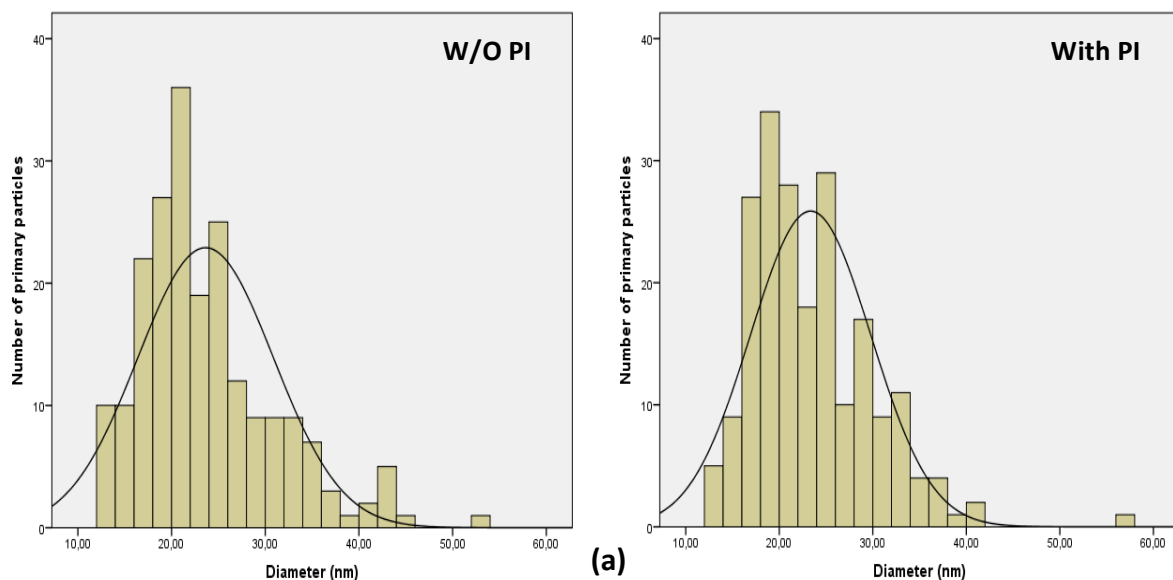
249 **Figure 6.** Fractal dimensions of particulate matter from the HR-TEM images.

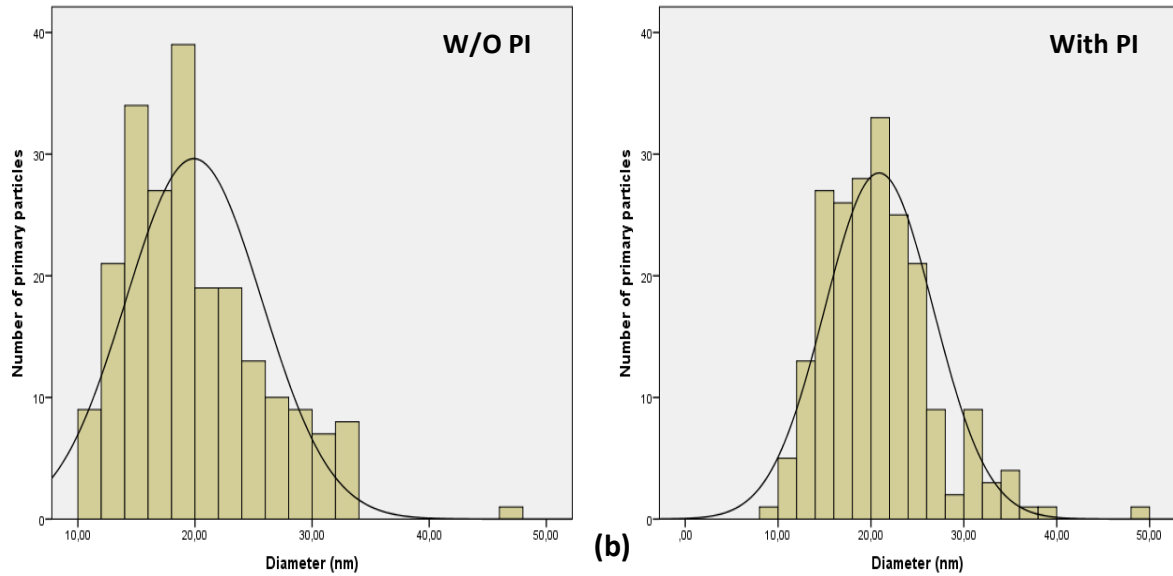
250 The primary particle diameter (d_{p0}) size distribution for both fuels with or without post-
 251 injection has been measured by selecting around 200 primary particles (more than 33 HR-TEM
 252 photographs for each condition and fuel) in order to fit normal distribution as shown in Figure 7. In
 253 Figure 7, the maximum number concentration, MMD, and sigma g for each condition and fuel are
 254 shown in Table 4. Figure 8 shows smaller size primary particles from the combustion of B20 for
 255 both injection setting (with and without post-injection) compared to diesel primary particles due to
 256 lower rate of production of soot precursors, soot formation and soot growth, and to the increase soot
 257 oxidation during the combustion of oxygenated fuel [16]. This result is in agreement with results
 258 obtained from biodiesel fuel [55] and butanol [16, 56] fuel blends without post-injection using other
 259 engine technologies [16, 56]. The size of primary particles is slightly reduced when post-injection
 260 was used for both fuels (Figure 8). It is believed this is due to an enhancement in the soot oxidation
 261 rate in the expansion stroke under post-injection conditions.

262 **Table 4.** Maximum number concentration, MMD and sigma g for diesel fuel and B20.

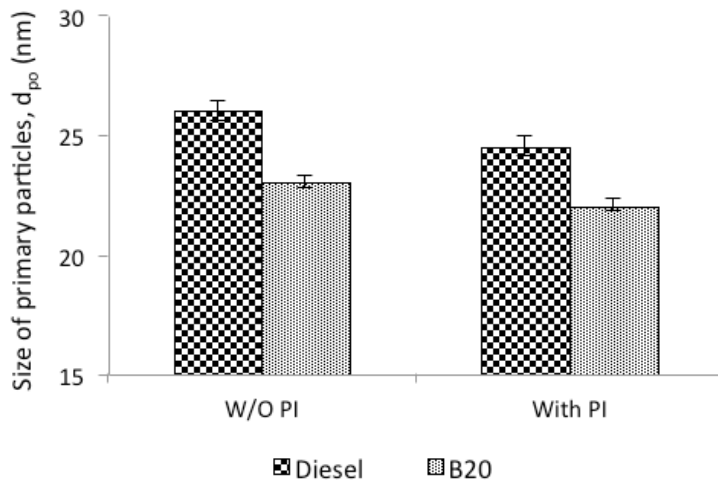
	Diesel W/O PI	Diesel with PI	B20 W/O PI	B20 with PI
Max. number concentration	29.04	28.87	26.41	24.12
MMD (nm)	25	24	23	21
Sigma g	7.25	6.45	5.86	5.82

263





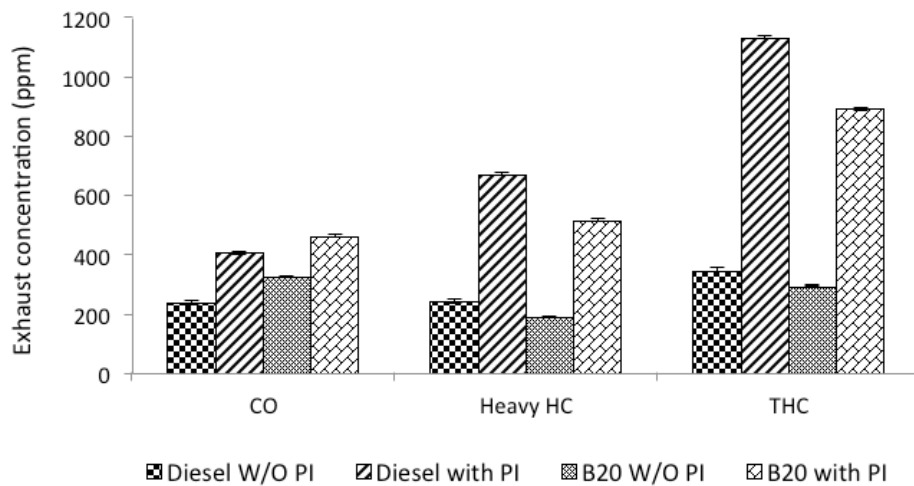
264 **Figure 7.** Primary particles size distributions for (a) diesel fuel, and (b) B20.



265
266 **Figure 8.** Average size of primary particles (d_{po}) for diesel and B20.

267 Figure 9 shows the CO, heavy HC, and THC engine-out emissions for the two studied fuels
 268 at both injection strategies. It can be noticed that THC emissions were lower from the combustion of
 269 the alcohol blend (B20) for both injection strategies. The higher HC emissions observed with diesel
 270 can be attributed to several reasons including absence of oxygen in the fuel molecule, and less
 271 efficient oxidation. The THC emissions in the case of post-injection are much higher compared to
 272 the case without post-injection. This confirms that the quantity and timing chosen for the post-
 273 injection allows to keep most of them unburnt and available to be oxidised in the DOC. Yamamoto,
 274 et al. and Chen, [26, 30] reported that the late post-injection lead to high level of THC emissions. It
 275 is reported that the reason of the increase in CO emissions observed for B20, especially without
 276 post-injection, can be attributed to the expected lower local in-cylinder temperature (Figure 2) and
 277 less CO oxidation during the combustion process due to the higher enthalpy of vaporisation of

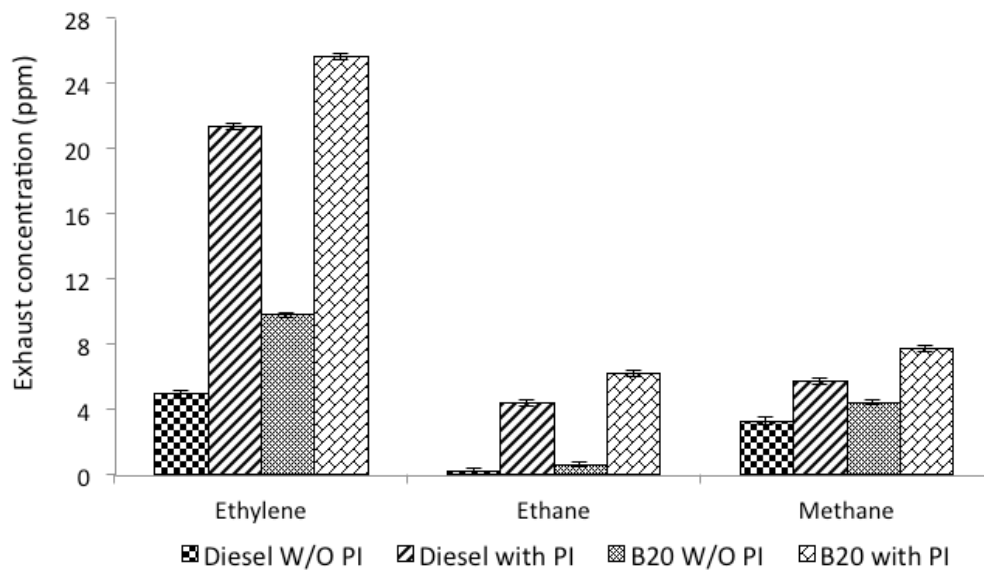
278 butanol with respect to diesel fuel [27]. Therefore, it seems that at this engine load operation the
 279 oxygen content and high reactivity of the butanol molecule enables to partially oxidise most of the
 280 HC species to CO, but the colder in-cylinder conditions due to the enthalpy of vaporization of
 281 butanol hinders the complete oxidation from CO to CO₂.



282

283 **Figure 9.** Engine exhaust gaseous emissions.

284 The concentration of HC species in the engine exhaust upstream the catalyst differs for diesel
 285 and B20 engine fuelling (Figure 10). The concentration of the light HC species studied including
 286 saturated (methane, ethane) and unsaturated (ethylene) species is higher for B20 with respect to
 287 diesel fuel combustion, conversely to the THC emissions presented earlier. It is thought that this is
 288 due to the thermal decomposition of the butanol component to light HC species and CO rather than
 289 forming heavy HC components as in the case of diesel fuel combustion. The level of HC emissions
 290 was lower from the combustion of B20 compared to the diesel fuel combustion. This can be due to
 291 improved combustion efficiency of the fuel in the presence of oxygen in the fuel as has also been
 292 described in [56] and due to the combustion patterns described in Figure 2, where a small increase in
 293 the in-cylinder pressure was obtained. From the results it can be also observed that with the
 294 incorporation of the fuel post-injection, higher concentration of the total and selected HC species
 295 were measured for both fuels due to the late timing of the post-injection [26].



296

297 **Figure 10.** Engine exhaust hydrocarbon species measured upstream the DOC.

298

299

300

301

302

303

304

305

306

307

308

309

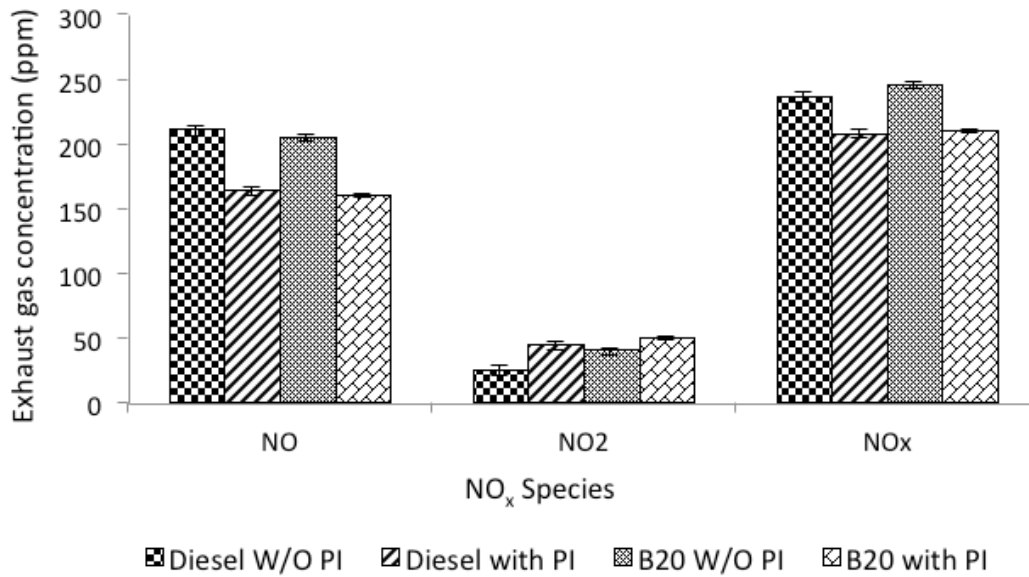
310

311

312

313

A slight increase in NO_x ($\text{NO} + \text{NO}_2$) was measured for the B20 combustion with respect to diesel combustion for both injection strategies (Figure 11). This can be due to the slight increase of in-cylinder pressure as seen in Figure 2 and the presence of the chemically bound oxygen content in B20 as it has been previously reported in the case of oxygenated fuels [56]. In addition, the oxygen content and lower cetane number of butanol enhanced the burning rate (faster burning). Chen et al [57] reported similar trends in NO_x emissions from the combustion of n-butanol-diesel blends and suggested that this was a result of the increased ignition delay that was then led to wider high-temperature combustion region. In addition, the oxygen content and lower cetane number of butanol enhanced the burning rate (faster burning). Although both fuels have similar NO concentration, it seems that B20 blend has higher oxidation from NO to NO_2 than diesel fuel due to the oxygen in the molecule. When post-injection was utilised the emissions of NO were decreased with simultaneously increasing in NO_2 for both fuels (Figure 11). This is can be explained because a portion of NO was oxidised to NO_2 by hydroperoxy radical (HO_2) formed during post combustion [58] and because of the reduction of NO_x with some of the HCs post-injected. It was noted that the engine out NO_x emissions decreased under post-injection due to the possible formation of nitrated-hydrocarbon by reacting NO_x with radical HC [58].



314

315 **Figure 11.** NO_x species concentrations of each gas species for with and without post-injection.

316 **3.3 Brake specific fuel consumption and brake thermal efficiency**

317 The brake specific fuel consumption (BSFC) and brake thermal efficiency (BTE) for both
 318 diesel and butanol blends are summarized in Table 5. It was noticed that post injection strategy
 319 increased the brake specific fuel consumption (BSFC) compared to that of main injection for both
 320 fuels. Moreover, BSFC slightly increased with B20 for both injection strategies when compared to the
 321 diesel fuel. The mean increase in BSFC for B20 when compared to the diesel under the same
 322 condition is 0.02811 and 0.02903 kg/kWh for without post-injection and with post-injection
 323 respectively. This is due to the lower calorific value recorded for B20 (see Table 2) compared to the
 324 diesel fuel. Lapuerta et al. [59] and Hajbabaei et al. [60] reported that the oxygenated fuels increases
 325 the BSFC mainly due to the reduced calorific value when compared to the diesel. Furthermore, the
 326 smaller increase in BSFC for B20 its compensated by its lower calorific value resulting in an increase
 327 in brake thermal efficiency. This could be due to the oxygen content in the B20 that improves the
 328 combustion efficiency and this is consistent with other researchers cited in introduction. It is clear
 329 from Table 5 that the post-injection reduce brake thermal efficiency and increase the exhaust gas
 330 temperature (EGT) for both fuels.

331

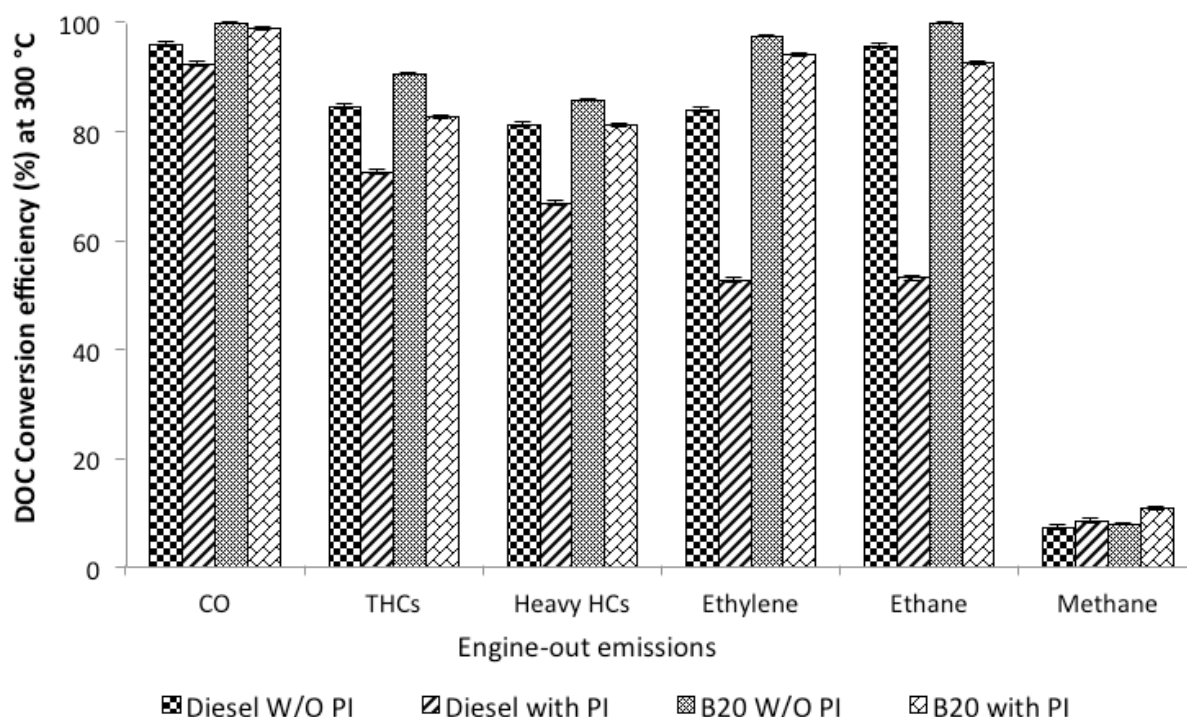
Table 5. Brake specific fuel consumption and thermal efficiency.

Fuel Parameters	Diesel fuel		B20	
	W/O PI	With PI	W/O PI	With PI
Brake specific fuel consumption, BSFC (kg/kWh)	0.3484	0.3645	0.3765	0.3935
Exhaust gas temperature, EGT (°C)	283	291	272	284
Brake thermal efficiency (BTE)	23.97	23.25	25.44	24.83

332 3.4 Influence of fuel post-injection and fuel properties on DOC activity

333 Combustion by-products in the exhaust gas are competing with each other to be adsorbed
334 into the active sites of the catalyst [16, 22], effects that is highly depends on the temperature, flow
335 conditions, space velocity and concentration and nature of the exhaust species. In active control
336 aftertreatments such as diesel particulate filters (DPFs) the ability of the DOC to effectively oxidise
337 the fuel and hydrocarbons and provide the required heat is important for the efficient operation of the
338 engine system (including aftertreatment and engine fuel economy and emissions). The gas hourly
339 space velocity (GHSV) and temperature of the DOC in this study were controlled and set at 35000 h⁻¹
340 and 300 °C, respectively in order to isolate the effect of exhaust gas composition.

341 The DOC is very effective in reducing CO in the engine exhaust from the combustion of both
342 fuels, with the catalyst's CO conversion efficiency being higher for B20 blend. In the case of post-
343 injection, the catalyst's CO oxidation efficiency was reduced (Figure 12), this is due to increased
344 concentration of species that are now competing for the same number of active sites. The HC species
345 presented in Figure 12 are light saturated (methane, ethane), light unsaturated (ethylene) and heavy
346 HCs. The results confirm the differences in reactivity of the hydrocarbon species. Methane (CH₄) as
347 a short chain saturated hydrocarbon was the most difficult component to oxidise in the catalyst due
348 to its low oxidation reactivity [23, 61]. Particularly, it can be observed that the conversion efficiency
349 of methane over the catalyst was even lower than 10% at 300 °C for all the conditions studied. In
350 addition, the increased concentration of heavier HCs and fuel in the exhaust that reaches the DOC
351 leads to its non-selective poisoning (i.e. fouling or masking). The catalyst active sites are now
352 occupied by the increased concentration of HCs and fuel that are interfering with the reactants
353 transport phenomena to the catalyst active sites. This non-selective poisoning limits the catalytic
354 surface area and obstructs access of the reactants to the pores. In this case the effect is reversible as
355 for the B20 fuel combustion, the catalyst has the highest HC conversion efficiency at 300 °C
356 compared with diesel fuel (Figure 12). This could be due to several reasons such as lower
357 concentration of HC upstream the catalyst, higher reactivity of butanol and its derivatives, higher
358 level of NO₂ emissions to catalytically oxidise the HC species [16, 62], lower PM/soot levels that
359 can be responsible for blocking the active sites.



360

361

Figure 12. DOC activity at 300 °C.

362 4. Conclusions

363 The effect of fuel post-injection and butanol-diesel fuel blends (B20) on PM characteristics
 364 (including size, fractal dimension, radius of gyration, and size of primary particles) and gaseous
 365 emissions were analysed and their influence on DOC activity was investigated at exhaust
 366 temperature of 300 °C. Due to reduced PM number concentration and HC emissions from the
 367 combustion of B20 the catalyst activity was improved. The HR-TEM analysis showed that the
 368 number of primary particles of PM agglomerates emitted from B20 combustion was lower than that
 369 from the combustion of diesel fuel. As B20 has oxygen-containing compounds, they contribute to
 370 inhibit the rate of soot formation and to increase the rate of oxidation, resulting in particles with
 371 smaller average size and fractal dimension. It is observed that the fuel post-injection has more clear
 372 benefits on PM reduction, resulting in enhanced soot oxidation with similar trends on the
 373 morphology of agglomerates as the presence of oxygenated compounds. HR-TEM analysis supports
 374 the results from SMPS and revealed that B20 produces particles with smaller average size compared
 375 to diesel fuel.

376 The fuel components as has been highlighted from the use of primary alcohols in this study,
 377 can improve engine systems performance by providing a chain of beneficial effects; from the
 378 combustion process to emissions formation processes to their abatement processes in the
 379 aftertreatment systems. In this case the changes in fuels properties from the incorporation of butanol

380 into diesel fuel, led to cleaner combustion that eased species (i.e. HCs/fuel and engine out emissions)
381 oxidation in the DOC. These trends will favour the active control strategies in the aftertreatment
382 systems and will positively impact on their performance (i.e. increase activity, improve durability)
383 and overall engine fuel economy.

384 **5. Acknowledgements**

385 Special thanks to the to the Iraqi government and Ministry of Higher Education and Scientific
386 Research in Baghdad, Iraq for providing PhD scholarship and maintenance grant for M.A. Fayad.
387 Innovative UK (*The Technology Strategy Board*, TSB) and EPSRC (*Engineering and Physical*
388 *Science Research Council*) acknowledged for funding/supporting this work with the projects CREO
389 ref 400176/149 and EP/G038139/1, respectively. Johnson Matthey is acknowledged for providing
390 the catalysts. F.J. Martos expresses thanks to the government of Spain for supporting his research
391 stay with reference PRX15/00256 at University of Birmingham. D. Fernández-Rodríguez expresses
392 thanks to the University of Castilla-La Mancha (Spain) for supporting his research stay at the
393 University of Birmingham. With thanks to Advantage West Midlands and the European Regional
394 Development Fund, funders of the Science City Research Alliance Energy Efficiency project-a
395 collaboration between the Universities of Birmingham and Warwick.

396 **ABBREVIATIONS**

397 aTDC = after top dead centre
398 B20D80 = butanol 20 %, and diesel 80%
399 bTDC = before top dead centre
400 BSFC = brake specific fuel consumption
401 CAD = crank angle degree
402 CI = compression ignition
403 CO = carbon monoxide
404 CO₂ = carbon dioxide
405 d_{p0} = size of primary particles
406 DOC = diesel oxidation catalyst
407 DPF = diesel particulate filter
408 EGT = exhaust gas temperature
409 GHSV = gas hourly space velocity
410 HC = hydrocarbons
411 IMEP = indicated mean effective pressure
412 NO = nitric oxide
413 NO₂ = nitrogen dioxide
414 NO_x = nitrogen oxides

415 n_{po} = number of primary particles
416 R_g = radius of gyration
417 SMPS = scanning mobility particle sizer
418 PSD = particulate size distribution
419 PI = post-injection
420 PM = particulate matter
421 TEM = transmission electron microscopy
422 THC = total hydrocarbons
423 ULSD = ultra low sulfur diesel
424 M-I = main injection
425 W/O PI = without post-injection
426 BTE = brake thermal efficiency

427 **6. References**

- 428 1. Bouchez, M., Dementhon, J. B., *Strategies for the control of particulate trap regeneration*.
429 2000, SAE technical paper.
- 430 2. Gill, S.S., Chatha, G. S., Tsolakis, A., *Analysis of reformed EGR on the performance of a diesel*
431 *particulate filter*. international journal of hydrogen energy, 2011. **36**(16): p. 10089-10099.
- 432 3. Zhu, L., Z. Huang, and J. Fang, *The Effects of Diesel Oxidation Catalyst on Particulate Emission*
433 *of Ethanol-Biodiesel Blend Fuel*. 2014, SAE Technical Paper.
- 434 4. Sukjit, E., Herreros, J. M., Dearn, K. D., Garcia-Contreras, R., Tsolakis, A., *The effect of the*
435 *addition of individual methyl esters on the combustion and emissions of ethanol and butanol*
436 *-diesel blends*. Energy, 2012. **42**(1): p. 364-374.
- 437 5. Koivisto, E., Ladommatos, N., Gold, M., *Systematic study of the effect of the hydroxyl*
438 *functional group in alcohol molecules on compression ignition and exhaust gas emissions*.
439 Fuel, 2015. **153**: p. 650-663.
- 440 6. Zhang, Z., Balasubramanian, R., *Investigation of particulate emission characteristics of a*
441 *diesel engine fueled with higher alcohols/biodiesel blends*. Applied Energy, 2016. **163**: p. 71-
442 80.
- 443 7. Mwangi, J.K., Lee, W., Chang, Y., Chen, C., Wang, L., *An overview: Energy saving and*
444 *pollution reduction by using green fuel blends in diesel engines*. Applied Energy, 2015. **159**.
- 445 8. Bermudez, V., Lujan, J.M., Pla, B., Linares, W.G., *Comparative study of regulated and*
446 *unregulated gaseous emissions during NEDC in a light-duty diesel engine fuelled with Fischer*
447 *Tropsch and biodiesel fuels*. Biomass and Bioenergy, 2011. **35**.
- 448 9. Lapuerta, M., Armas, O., Herreros, J.M., *Emissions from a diesel-bioethanol blend in an*
449 *automotive diesel engine*. Fuel, 2008. **87**: p. 25-31.
- 450 10. Hellier, P., Ladommatos, N., Allan, R., Rogerson, J., *The Influence of Fatty Acid Ester Alcohol*
451 *Moiety Molecular Structure on Diesel Combustion and Emissions*. Energy & fuels, 2012. **26**: p.
452 1912-1927.
- 453 11. Eveleigh, A., Ladommatos, N., Hellier, P., Jourdan, A., *An investigation into the conversion of*
454 *specific carbon atoms in oleic acid and methyl oleate to particulate matter in a diesel engine*
455 *and tube reactor*. Fuel, 2015. **153**: p. 604-611.
- 456 12. Xing-cai, L., Jian-Guang, Y., Wu-Gao, Z., Zhen, H., *Effect of cetane number improver on heat*
457 *release rate and emissions of high speed diesel engine fueled with ethanol-diesel blend fuel*.
458 Fuel, 2004. **83**(14): p. 2013-2020.

- 459 13. Zoldy, M., A. Hollo, and A. Thernesz, *Butanol as a diesel extender option for internal*
460 *combustion engines*. 2010, SAE Technical Paper.
- 461 14. Armas, O., García-Contreras, R., Ramos, Á., *Pollutant emissions from New European Driving*
462 *Cycle with ethanol and butanol diesel blends*. Fuel Processing Technology, 2014. **122**: p. 64-
463 71.
- 464 15. Lapuerta, M., Armas, O., García-Contreras, R. , *Effect of Ethanol on Blending Stability and*
465 *Diesel Engine Emissions*. Energy & fuels, 2009. **23**(9): p. 4343-4354.
- 466 16. Fayad, M.A., Herreros, J. M., Martos, F. J., Tsolakis, A., *Role of Alternative Fuels on*
467 *Particulate Matter (PM) Characteristics and Influence of the Diesel Oxidation Catalyst*.
468 Environmental science & technology, 2015. **49**(19): p. 11967-11973.
- 469 17. López, A.F., Cadrazco, M., Agudelo, A. F., Corredor, L. A., Vélez, J. A., Agudelo, J. R., *Impact of*
470 *n-butanol and hydrous ethanol fumigation on the performance and pollutant emissions of an*
471 *automotive diesel engine*. Fuel, 2015. **153**: p. 483-491.
- 472 18. Rakopoulos, D.C., Rakopoulos, C. D., Giakoumis, E. G., Dimaratos, A. M., Kyritsis, D. C., *Effects*
473 *of butanol–diesel fuel blends on the performance and emissions of a high-speed DI diesel*
474 *engine*. Energy Conversion and Management, 2010. **51**(10): p. 1989-1997.
- 475 19. Rakopoulos, D.C., Rakopoulos, C. D., Papagiannakis, R. G., Kyritsis, D. C., *Combustion heat*
476 *release analysis of ethanol or n-butanol diesel fuel blends in heavy-duty DI diesel engine*.
477 Fuel, 2011. **90**(5): p. 1855-1867.
- 478 20. Rounce, P., A. Tsolakis, and A. York, *Speciation of particulate matter and hydrocarbon*
479 *emissions from biodiesel combustion and its reduction by aftertreatment*. Fuel, 2012. **96**: p.
480 90-99.
- 481 21. Ye, S., Yap, Y. H., Kolaczkowski, S. T., Robinson, K., Lukyanov, D., *Catalyst ‘light-*
482 *off’ experiments on a diesel oxidation catalyst connected to a diesel engine—Methodology*
483 *and techniques*. Chemical Engineering Research and Design, 2012. **90**(6): p. 834-845.
- 484 22. Lefort, I., Herreros, J. M., Tsolakis, A., *Reduction of low temperature engine pollutants by*
485 *understanding the exhaust species interactions in a diesel oxidation catalyst*. Environmental
486 science & technology, 2014. **48**(4): p. 2361-2367.
- 487 23. Herreros, J.M., Gill, S. S., Lefort, I., Tsolakis, A., Millington, P., Moss, E., *Enhancing the low*
488 *temperature oxidation performance over a Pt and a Pt–Pd diesel oxidation catalyst*. Applied
489 Catalysis B: Environmental, 2014. **147**: p. 835-841.
- 490 24. Mittendorfer, F., Thomazeau, C., Raybaud, P., Toulhoat, H., *Adsorption of unsaturated*
491 *hydrocarbons on Pd (111) and Pt (111): A DFT study*. The Journal of Physical Chemistry B,
492 2003. **107**(44): p. 12287-12295.
- 493 25. Meakin, P., Donn, B., Mulholland, G. W., *Collisions between point masses and fractal*
494 *aggregates*. Langmuir, 1989. **5**(2): p. 510-518.
- 495 26. Yamamoto, K., Takada, K., Kusaka, J., Kanno, Y., Nagata, M. *Influence of diesel post injection*
496 *timing on HC emissions and catalytic oxidation performance*. in *Powertrain and Fluid Systems*
497 *Conference and Exhibition*. 2006.
- 498 27. Chen, P., Ibrahim, Umar, Wang, Junmin, *Experimental investigation of diesel and biodiesel*
499 *post injections during active diesel particulate filter regenerations*. Fuel, 2014. **130**: p. 286-
500 295.
- 501 28. Desantes, J., Bermúdez, V, Pastor, JV, Fuentes, E, *Investigation of the influence of post-*
502 *injection on diesel exhaust aerosol particle size distributions*. Aerosol science and technology,
503 2006. **40**(1): p. 80-96.
- 504 29. O'Connor, J., and Musculus, M., *Post Injections for Soot Reduction in Diesel Engines - A*
505 *Review of Current Understanding*. SAE Technical Paper, 2013: p. 01-0917.
- 506 30. Chen, S.K., *Simultaneous reduction of NOx and particulate emissions by using multiple*
507 *injections in a small diesel engine*. 2000, SAE Technical Paper.
- 508 31. Sperl, A., *The Influence of Post-Injection Strategies on the Emissions of Soot and Particulate*
509 *Matter in Heavy Euro V Diesel Engine*. SAE Technical Paper , 2011. **36**(0350).

- 510 32. Bobba, M., Musculus, M., Neel, W., *Effect of post injections on in-cylinder and exhaust soot*
511 *for low-temperature combustion in a heavy-duty diesel engine*. SAE International Journal of
512 Engines, 2010. **3**(1): p. 496-516.
- 513 33. Yun, H., Reitz, R. D., *An experimental investigation on the effect of post-injection strategies*
514 *on combustion and emissions in the low-temperature diesel combustion regime*. Journal of
515 Engineering for Gas Turbines and Power, 2007. **129**(1): p. 279-286.
- 516 34. Barro C., T.F., Obrecht P., Boulouchos K. *Influence of post-injection parameters on soot*
517 *formation and oxidation in a common-rail-diesel engine using multi-color-pyrometry*. in
518 *ASME 2012 internal combustion engine division fall technical conference*. 2012. American
519 Society of Mechanical Engineers.
- 520 35. Desantes, J.M., Arrègle, J., López, J. J., García, A., *A comprehensive study of diesel*
521 *combustion and emissions with post-injection*. 2007, SAE Technical Paper.
- 522 36. Poorghasemi, K., Ommi, F., Yaghmaei, H., Namaki, A., *An investigation on effect of high*
523 *pressure post injection on soot and NO emissions in a DI diesel engine*. Journal of mechanical
524 science and technology, 2012. **26**(1): p. 269-281.
- 525 37. Mohan B, Y.W.a.C.S., *Fuel injection strategies for performance improvment and emissions*
526 *reduction in compression ignition engines - A review*. Renewable and Sustainable Energy
527 Reviews, 2013. **28**: p. 664-676.
- 528 38. Valentino, G., Iannuzzi, S. E., Marchitto, L., Merola, S. S., Tornatore, C., *Optical Investigation*
529 *of Postinjection Strategy Effect at the Exhaust Line of a Light-Duty Diesel Engine Supplied*
530 *with Diesel/Butanol and Biodiesel Blends*. Journal of Energy Engineering, 2013. **140**(3): p.
531 A4014010.
- 532 39. Fino, D., *Diesel emission control: Catalytic filters for particulate removal*. Science and
533 Technology of Advanced Materials, 2007. **8**(1): p. 93-100.
- 534 40. Li, X., Guan, C., Luo, Y., Huang, Z., *Effect of multiple-injection strategies on diesel engine*
535 *exhaust particle size and nanostructure*. Journal of Aerosol Science, 2015. **89**: p. 69-76.
- 536 41. Yehliu, K., Armas, O., Vander W., Randy L., Boehman, A. L., *Impact of engine operating*
537 *modes and combustion phasing on the reactivity of diesel soot*. Combustion and Flame,
538 2013. **160**(3): p. 682-691.
- 539 42. Hiranuma, S., Takeda, Y., Kawatani, T., Doumeki, R., Nagasaki, K., Ikeda, T., *Development of*
540 *DPF System for Commercial Vehicle-Basic Characteristic and Active Regenerating*
541 *Performance*. 2003, SAE Technical Paper.
- 542 43. Parks, J., James, E., Huff, S. P., Kass, M. D., Storey, J. M., *Characterization of in-cylinder*
543 *techniques for thermal management of diesel aftertreatment*. 2007, Oak Ridge National
544 Laboratory (ORNL); Fuels, Engines and Emissions Research Center.
- 545 44. AVL, *Pressure Sensor for Combustion Analysis – Data Sheet GH13P [Internet]*. [Cited 3
546 November 2015]. Available from URL:
547 https://www.avl.com/documents/10138//885983//AT3368E_GH13P.pdf, 2011.
- 548 45. AVL, *Microifem Piezo 4th Generation – Piezo Amplifier [Internet]* [Cited 3 November 2015].
549 Available from URL: <https://www.avl.com/documents/10138//0//MicroIFEM+4P4+Piezo.>,
550 2013.
- 551 46. Lapuerta, M., Martos, F. J., Martín-González, G., *Geometrical determination of the lacunarity*
552 *of agglomerates with integer fractal dimension*. Journal of colloid and interface science,
553 2010. **346**(1): p. 23-31.
- 554 47. Lapuerta, M.B., R.; Martos, F. J., *A method to determine the fractal dimension of diesel soot*
555 *agglomerates*. J. Colloid Interface Sci., 2006. **303**: p. 149-158.
- 556 48. Westbrook, C.K., W.J. Pitz, and H.J. Curran, *Chemical kinetic modeling study of the effects of*
557 *oxygenated hydrocarbons on soot emissions from diesel engines*. The journal of physical
558 chemistry A, 2006. **110**(21): p. 6912-6922.

- 559 49. Choi, B., Jiang, Xiaolong, *Individual hydrocarbons and particulate matter emission from a*
560 *turbocharged CRDI diesel engine fueled with n-butanol/diesel blends*. Fuel, 2015. **154**: p. 188-
561 195.
- 562 50. Lee, K.O., Sekar, R., Choi, M. Y., Kang, J. S., Bae, C. S., Shin, H. D., *Morphological investigation*
563 *of the microstructure, dimensions, and fractal geometry of diesel particulates*. Proceedings of
564 the Combustion Institute, 2002. **29**(1): p. 647-653.
- 565 51. Lee, K.O., Cole, R., Sekar, R., Choi, M. Y., Z., J., Kang, J., Bae, C., *Detailed characterization of*
566 *morphology and dimensions of diesel particulates via thermophoretic sampling*. 2001, SAE
567 Technical Paper.
- 568 52. Crookes, R.J., Sivalingam, G., Nazha, M. A. A, Rajakaruna, H., *Prediction and measurement of*
569 *soot particulate formation in a confined diesel fuel spray-flame at 2.1 MPa*. International
570 journal of thermal sciences, 2003. **42**(7): p. 639-646.
- 571 53. Choi, S.C.R., Hyun G. u., Lee, K. S., Lee, C. S., *Effects of fuel injection parameters on the*
572 *morphological characteristics of soot particulates and exhaust emissions from a light-duty*
573 *diesel engine*. Energy & Fuels, 2010. **24**(5): p. 2875-2882.
- 574 54. Park, K.K., D. B.; McMurry, P. H., *Structural properties of diesel exhaust particles measured*
575 *by transmission electron microscopy (TEM): Relationships to particle mass and mobility*.
576 Aerosol Science and Technology, 2004. **38**(9): p. 881-889.
- 577 55. Hwang, J.J., Y., Bae, C. *Particulate morphology of waste cooking oil biodiesel and diesel in a*
578 *heavy duty diesel engine*. in *International Conference on Optical Particle Characterization*
579 *(OPC 2014)*. 2014. International Society for Optics and Photonics.
- 580 56. Qu, L., Wang, Z., Hu, H., Li, X., Zhao, Y. , *Effects of butanol on components and morphology of*
581 *particles emitted by diesel engines*. Research of Environmental Sciences, 2015. **28**(10): p.
582 1518-1523.
- 583 57. Chen, Z., Wu, Z., Liu, J., Lee, C., *Combustion and emission characteristics of high n-*
584 *butanol/diesel ratio blend in a heavy duty diesel engine and EGR impact*. energy Conversion
585 and Management, 2014. **78**: p. 787-795.
- 586 58. Richard K., L., J. Cole, A.. "A reexamination of the Rapre NOx process" . Combustion and
587 Flame, 1990. **82**(3-4): p. 435-443.
- 588 59. Lapuerta, M., Armas, O., Rodríguez-Fernández, J., *Effect of biodiesel fuels on diesel engine*
589 *emissions*. Progress in Energy and Combustion Science, 2008. **34**: p. 198-223.
- 590 60. Hajbabaie, M., Johnson, K.C., Okamoto, R., Durbin, T.D., *Evaluation of the Impacts of Biofuels*
591 *on Emissions for a California Certified Diesel Fuel from Heavy-Duty Engines*. SAE Technical
592 Paper, 2013: p. 01-1138m.
- 593 61. Diehl, F., Barbier, J., Duprez, D., Guibard, I., Mabilon, G., *Catalytic oxidation of heavy*
594 *hydrocarbons over Pt/Al₂O₃. Influence of the structure of the molecule on its reactivity*.
595 Applied Catalysis B: Environmental, 2010. **95**(3): p. 217-227.
- 596 62. Lapuerta, M., García-Contreras, R., Campos-Fernández, J., Dorado, M. P., *Stability, lubricity,*
597 *viscosity, and cold-flow properties of alcohol– diesel blends*. Energy & fuels, 2010. **24**(8): p.
598 4497-4502.

599